*R*esearch in
*A*stronomy and
*A*strophysics

Brightness temperature for 166 radio sources [*]

Jun-Hui Fan[1,2], Yong Huang[1], Yu-Hai Yuan[3,1], Jiang-He Yang[4], Yi Liu[1], Jun Tao[5], Ying Gao[1], Tong-Xu Hua[1], Rui-Guang Lin[1], Jiang-Shui Zhang[1], Jing-Yi Zhang[1] and Yi-Ping Qin[1]

[1] Center for Astrophysics, Guangzhou University, Guangzhou 510006, China;
jhfan_cn@yahoo.com.cn
[2] Physics Institute, Hunan Normal University, Changsha 410081, China
[3] Center for Astrophysics, University of Science and Technology of China, Hefei 230026, China
[4] Department of Physics and Electronics Science, Hunan University of Arts and Science, Changde 415000, China
[5] Shanghai Astronomical Observatory, Chinese Academy of Sciences, Shanghai 200030, China

Abstract   Using the database of the University of Michigan Radio Astronomy Observatory (UMRAO) at three radio frequencies (4.8, 8 and 14.5 GHz), we determined the short-term variability timescales for 166 radio sources. The timescales are 0.15 d (2007+777) to 176.17 d (0528–250) with an average timescale of $\Delta t_{\rm obs} = 17.1 \pm 16.5$ d for the whole sample. The timescales are used to calculate the brightness temperatures, $T_{\rm B}$. The value of $\log T_{\rm B}$ is in the range of $\log T_{\rm B} = 10.47$ to 19.06 K. In addition, we also estimated the boosting factor for the sources. The correlation between the polarization and the Doppler factor is also discussed.

Key words: galaxies: active — BL Lacertae objects: general — galaxies: jets

1 INTRODUCTION

Blazars form an extreme subclass of Active Galactic Nuclei (AGNs), showing high and variable luminosity, superluminal motions in their radio components, high gamma-ray emission, high polarization, etc. (e.g. Aller et al. 1992, 1999, 2003; Andruchow et al. 2005; Cellone et al. 2007; Ciprini et al. 2007; Efimov et al. 2002; Fan et al. 2004; Fan 2005a,b; Fan et al. 1996; Gupta et al. 2004; Romero et al. 2002; Sambruna et al. 2000; Wills et al. 1992). Based on the observational properties, the blazar group can be divided into two subclasses (BL Lacertae objects – BLs and flat spectrum radio quasars – FSRQs). BLs have violent variability on timescales from hours to years at frequencies from radio to γ-rays (see Fan 2005b), and almost no emission lines. There are also some emission lines found from BLs, like BL Lacertae (2200+420) found with emission lines of Hα and Hβ in 1995 (Vermeulen et al. 1995). FSRQs include highly polarized quasars (HPQs), optically violent variable quasars (OVVs), and core-dominated quasars (CDQs). The observational properties of BLs are quite similar to those of FSRQs except for their emission line properties. FSRQs show strong emission lines whereas BLs show weak emission lines or even no emission lines at all.

The extreme observational properties of these sources are explained by the beaming effect. Due to beaming, emissions from the jet appear strongly boosted in the observer's frame of reference: $F^{\rm ob} = \delta^p F^{\rm in}$, where $F^{\rm in}$ is the intrinsic emission in the source frame and $F^{\rm ob}$ is the observed luminosity, and δ is the Doppler boosting factor. The value of p depends on the shape of the emitted spectrum and the

detailed physics of the jet (Lind & Blandford 1985), $p = 3 + \alpha$ is for a moving compact source and $p = 2 + \alpha$ is for the case of a continuous jet, α is the spectral index. At the same time, the observed timescale is shortened by a factor δ, i.e. $\Delta t^{\rm ob} = \Delta t^{\rm in}/\delta$. $\Delta t^{\rm ob}$ and $\Delta t^{\rm in}$ are respectively the observed and the intrinsic variability timescales. The short timescale is a very useful parameter, which might put constraints on the size of the emitting region, i.e., $R \leq c\Delta t$. Short timescales are observed in all frequencies – from radio to TeV bands (see Dondi & Ghisellini 1995; Fan et al. 2004; Gaidos et al. 1996; Romero et al. 1994; Romero et al. 2002; Wagner & Witzel 1995; Witzel & Quirrenbach 1993; Xie et al. 2004).

However, short timescales are not available for a large sample. Fortunately, in the radio band, monitoring programs (UMRAO) provide a good basis for the investigation of short timescales. Therefore, we have used the UMRAO database to find the short term timescale. The paper is arranged as follows. In Section 2, the sample is presented and determination of short timescales and brightness temperature are discussed, while in Section 3, we give some discussions, and in Section 4, we present the conclusions.

2 SAMPLE AND RESULTS

2.1 Sample

UMRAO provides us with a very useful radio database (*http://www.astro.lsa.umich.edu/obs /radiotel /umrao.php*). From the UMRAO preliminary database, we get 166 radio sources for which light curves are available in three bands (4.8, 8 and 14.5 GHz). Out of 166 radio sources, 47 are BLs, 92 are FSRQs, 21 are galaxies—G, and 6 are unidentified. For these sources, we have looked for the existence of short term timescales.

2.2 Short-term Timescale

To find the short term timescale, we use the following process. For a certain source, there are three light curves at $\nu = 4.8$, 8 and 14.5 GHz, respectively. For each frequency, there are n sets of data (t_i, S_i), $i = 1, 2, ..., n$. Then we calculate the time difference (Δt_{jk}), the variability (ΔF_{jk}), and the standard deviation (σ_{jk}) between the jth set and the kth set of data.

$$\Delta t_{jk} = |t_j - t_k|, \quad \Delta F_{jk} = |F_j - F_k|, \quad \sigma_{jk} = \sqrt{\sigma_j^2 + \sigma_k^2}, \tag{1}$$

where j, $k = 1, 2, ..., n$, so, we have $n(n-1)/2$ sets of Δt_{jk}, ΔF_{jk} and σ_{jk}. Then, if $\Delta F_{jk} > 5\sigma_{jk}$, we select Δt_{jk} as the short term timescales at the frequency for the source. In this sense, there are three shortest timescales, $\Delta t_{4.8\,\rm GHz}$, $\Delta t_{8\,\rm GHz}$, and $\Delta t_{14.5\,\rm GHz}$ for each source. Finally, we use the shortest timescale amongst the three shortest timescales as the short term timescale for the source, namely $t_{\rm obs} = \min(\Delta t_{4.8\,\rm GHz}, \Delta t_{8\,\rm GHz}, \Delta t_{14.5\,\rm GHz})$. For illustration, we take the 8 GHz light curve of 0127+233; see Figure 1 as an example. The calculation is presented in Figure 2, from which we can observe that the shortest timescale corresponding to the criterion of $\Delta F_{jk} > 5\sigma_{jk}$ is 55.1 d, and the flux density variability is $\Delta F = 0.37$ Jy as shown in Figure 1. From our calculation, we find the timescales for the whole sample are in the range of 0.15 d (2007+777) to 176.2 d (0528–250) with an average timescale of $\Delta t_{\rm obs} = 17.1 \pm 16.5$ d.

2.3 Brightness Temperature

If we assume the timescale to be a measure of the size of the source, then the observed flux may be converted into a brightness temperature (Wagner & Witzel 1995)

$$T_{\rm B} = (4.5 \times 10^{10}\,{\rm K})\Delta F \left[\frac{\lambda d}{t_{\rm ob}(1+z)}\right]^2, \tag{2}$$

where ΔF is the variability of flux density in Jy, λ the wavelength in cm, d the distance in Mpc, and $t_{\rm obs}$ the timescale in d. From the available data as listed in Table 1, we have calculated the brightness
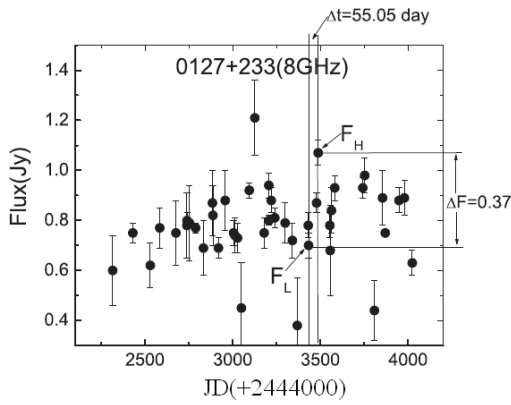
Fig. 1 Light curve of 0127+233 at 8 GHz. The vertical lines indicate the timescale of 55.1 d and the corresponding variability of $\Delta F = F1 - F2 = 0.37$ Jy.
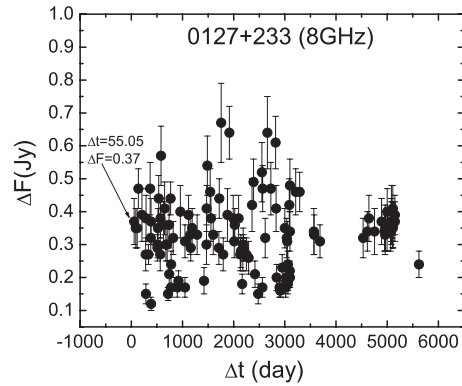
Fig. 2 Calculated result based on the light curves of 0127+233 at 8 GHz. The X-axis shows the time interval while the Y-axis indicates the corresponding variability.

temperature T_B for 166 sources. Redshifts are available in recent work for some redshift-unknown sources. That for 0355+508 is available in Agudo et al. (2007). Redshifts are also available in SDSS. Here, the average redshift value is taken as the redshift for the remaining sources whose redshifts are unknown. The average value is $\langle z \rangle = 0.35 \pm 0.30$ for galaxies (GALs), $\langle z \rangle = 0.42 \pm 0.37$ for BL Lac objects (BLs), $\langle z \rangle = 1.01 \pm 0.65$ for flat spectrum radio quasars (FSRQs), and $\langle z \rangle = 0.76 \pm 0.62$ for the whole sample. Therefore, $\langle z \rangle = 0.76$ is taken for the unidentified source (N). The brightness temperatures are thus obtained in the range: $\log T_B = 10.47$ K for 0315+416 to $\log T_B = 19.06$ K for 2223–052; see Col. (12) in Table 1 for details.

3 DISCUSSION

Blazars show extreme observational properties including variable and strong emission, high and variable polarization, and very high energy radiation reaching even TeV energies. Those properties are known to be associated with the relativistic beaming effect. Short timescales are believed to be a measure of the source size, therefore, it is a very important observational physical parameter. Xie et al. (1991) used the short timescale to get the Doppler boosting factor in the optical bands. Short timescales are also used for Doppler factor estimation in the gamma-ray bands (Dondi & Ghisellini 1995; Fan et al. 1999; Cheng et al. 1999; Fan 2005b).

3.1 Variability Timescales

Based on the UMRAO database, Aller et al. (2003) found that variability in radio is common in blazars. For the timescales in radio bands, Hughes et al. (1992) used the method of structure function analysis with the UMRAO database and found that there is not much difference between BLs and FSRQs in the timescales with an averaged timescale of 1.95 yr for BLs and 2.35 yr for FSRQs. Aller et al. (1999) analyzed the variability properties of 45 radio-selected BLs and found that a characteristic timescale is identifiable in only 1/3 of the BL Lacs, and that the polarized flux exhibits variability with timescales of months to a few years. Based on 7 yr of radio observations from the RATAN 600 radio-telescope, Kovalev & Kovalev (2006) made a timescale analysis and found that the sources show strong variability with flux density changes of more than 50% over timescales of more than 1 month.

It is reasonable that different methods can give different timescales. Sometimes, the same method can return different results if the method is adapted to different time coverage of the light curve.

Table 1 Data for 166 Radio Sources

Name	ID	$P_{8\,\mathrm{GHz}}^{\mathrm{Max}}$	$\sigma_{P_{8\,\mathrm{GHz}}^{\mathrm{Max}}}$	z	ΔT^D	ΔF	σ	F_{L}	F_{H}	ν	$\log T_{\mathrm{B}}$	δ
(B1950)		(%)	(%)		(d)	(Jy)		(Jy)	(Jy)	(GHz)	(K)	
(1)	(2)	(3)	(4)	(5)	(6)	(7)	(8)	(9)	(10)	(11)	(12)	(13)
0003–066	BL	7.15	3.35	0.347	2.98	0.54	0.07	2.58	3.12	8	16.67	8.6
0007+106	FSRQ	44.76	21.08	0.09	0.98	0.23	0.04	0.38	0.61	8	16.24	7.04
0016+731	FSRQ	66.45	23.55	1.781	1	0.19	0.04	1.18	1.37	4.8	18.53	20.27
0022+638	N	2.27	0.82		18.54	1.05	0.17	7.47	8.52	8	15.88	5.96
0040+517	GAL	5.07	2.62	0.174	4.57	0.32	0.04	1.13	1.45	14.5	15.05	4.07
0048–097	BL	21.51	7.28	0.2	1	0.54	0.11	1.51	2.05	8	17.22	11.07
0059+581	FSRQ	5.06	1.22	0.643	1.01	0.53	0.08	2.59	3.12	8	18.01	15.9
0106+013	FSRQ	9.9	3.76	2.107	0.97	0.29	0.04	1.63	1.92	4.8	18.81	23.04
0108+388	FSRQ	19.94	9.01	0.669	2.05	0.09	0.01	0.37	0.46	14.5	16.13	6.7
0109+224	BL	41.92	11.81		0.95	0.23	0.04	0.7	0.93	14.5	16.91	9.59
0127+233	FSRQ	19.35	12.22	1.459	55.05	0.37	0.07	0.7	1.07	8	14.81	3.65
0133+476	FSRQ	12.83	1.02	0.859	0.98	0.58	0.09	2.37	2.95	8	18.24	17.7
0134+329	FSRQ	10.15	2.14	0.367	0.93	0.29	0.04	1.66	1.95	14.5	16.94	9.72
0153+744	FSRQ	61.01	34.64	2.338	13.51	0.09	0.01	0.4	0.49	14.5	15.1	4.16
0202+149	FSRQ	5.2	2	0.833	0.96	0.28	0.04	2.52	2.8	14.5	17.41	12.07
0212+735	FSRQ	8.89	1.01	2.367	1.98	0.38	0.06	2.66	3.04	14.5	17.39	11.99
0215+015	BL	18.16	8.11	1.721	1.96	1.42	0.07	1.6	3.02	14.5	17.85	14.79
0218+357	FSRQ	23.94	8.02	0.686	2.99	0.33	0.04	0.99	1.32	14.5	16.38	7.52
0219+428	BL	12.52	8.94	0.444	12.55	0.21	0.03	0.84	1.05	14.5	14.67	3.41
0220+427	GAL	10.55	4.32	0.0215	2.01	0.25	0.04	0.71	0.96	14.5	13.93	2.43
0234+285	FSRQ	9.24	2.21	1.21	1.94	1.11	0.1	5.05	6.16	8	18.11	16.65
0235+164	BL	17.08	7.86	0.94	0.88	0.59	0.05	1.37	1.96	14.5	17.87	14.95
0300+470	BL	12.08	4.79	0.475	1.03	0.38	0.07	2.73	3.11	8	17.66	13.52
0306+102	FSRQ	50.7	24.37	0.863	1.98	0.23	0.04	0.6	0.83	14.5	16.71	8.76
0315+416	GAL	12.51	3.8	0.0255	71.96	0.08	0.01	0.56	0.64	14.5	10.47	0.5
0316+413	FSRQ	0.86	0.24	0.0172	1	3.47	0.61	28.58	32.05	8	16.01	6.33
0323+022	BL	99.03	30.81	0.13	166.55	0.22	0.04	0.1	0.32	8	12.05	1.02
0333+321	FSRQ	13.86	1.23	1.259	0.97	0.21	0.04	1.5	1.71	8	18.01	15.89
0336–019	FSRQ	12.64	2.98	0.852	1	0.43	0.05	1.71	2.14	4.8	18.53	20.25
0355+508	N	12.32	3.96	1.52	0.95	0.52	0.1	9.32	9.84	8	18.5	19.99
0404+768	GAL	14.62	3.77	0.5895	1.97	0.44	0.04	1.51	1.95	14.5	16.78	9.02
0420–014	FSRQ	5.83	1.33	0.915	1.01	0.69	0.09	2.24	2.93	4.8	18.77	22.57
0422+004	BL	45.25	19.48	0.031	1.98	0.27	0.04	0.55	0.82	8	14.81	3.64
0430+052	FSRQ	10.14	1.58	0.0331	0.73	0.51	0.08	2.2	2.71	14.5	15.49	4.98
0440–003	FSRQ	6.18	1.85	0.844	8.97	0.24	0.03	1.14	1.38	14.5	15.41	4.8
0454–234	FSRQ	10.97	2.48	1.003	10.6	0.38	0.07	1.45	1.83	8	16.07	6.52
0456–020	FSRQ	9.86	1.79		0.95	1.09	0.15	2.61	3.7	8	18.63	21.16
0518+165	FSRQ	9.86	1.79	0.759	0.95	1.09	0.15	2.61	3.7	8	18.47	19.69
0521-365	FSRQ	4.2	0.76	0.055	0.97	0.73	0.11	6.06	6.79	8	16.34	7.38
0528+134	FSRQ	6.35	0.56	2.067	2	1.16	0.11	5.39	6.55	14.5	17.82	14.58
0528–250	FSRQ	21.45	10.26	2.81	176.17	0.41	0.08	0.05	0.46	14.5	13.59	2.08
0538+498	FSRQ	4.13	1.19	0.545	0.99	0.29	0.05	2.24	2.53	14.5	17.14	10.69
0552+398	FSRQ	4.55	1.88	2.365	0.89	0.71	0.13	6.99	7.7	8	18.88	23.72
0605+480	GAL	67.63	11.21	0.2771	2.03	0.19	0.03	0.66	0.85	8	16.39	7.56
0605–085	FSRQ	9.53	3.38	0.872	0.9	0.29	0.05	3.05	3.34	8	18.02	16
0607–157	FSRQ	16.48	4.81	0.324	0.94	1.69	0.17	2.88	4.57	4.8	18.57	20.58
0710+439	FSRQ	16.22	4.31	0.518	1.98	0.34	0.06	1.06	1.4	8	17.1	10.45
0711+356	FSRQ	17.51	9.47	1.62	0.99	0.09	0.01	0.36	0.45	14.5	17.22	11.06
0716+714	BL	75.06	32.44	0.3	0.57	0.09	0.01	0.46	0.55	14.5	16.71	8.76
0723+679	FSRQ	30.6	10.73	0.846	1.05	0.23	0.04	0.72	0.95	4.8	18.21	17.49
0735+178	BL	13.07	6.7	0.424	1.01	0.52	0.05	2.43	2.95	4.8	18.18	17.2
0754+100	BL	15.25	2.73	0.66	0.92	0.19	0.02	1.24	1.43	8	17.66	13.54
0804+499	FSRQ	32.18	10.7	1.433	2	0.22	0.04	0.88	1.1	14.5	16.94	9.73
0808+019	BL	16.93	8.62	1.148	15.91	0.43	0.08	0.84	1.27	8	15.84	5.87
0809+483	FSRQ	6.51	3.91	0.871	2	0.16	0.03	1.22	1.38	14.5	16.55	8.14
0814+425	BL	10.91	1.71	0.2453	1.92	0.14	0.01	0.91	1.05	4.8	16.66	8.57
0818–128	BL	28.61	11.7		23.58	0.24	0.04	1.2	1.44	14.5	14.14	2.68
0829+046	BL	12.15	3.57	0.18	0.98	0.59	0.11	1.98	2.57	8	17.2	10.94

Table 1 — *Continued.*

Name (B1950) (1)	ID (2)	$P_{8\,\text{GHz}}^{\text{Max}}$ (%) (3)	$\sigma_{P_{8\,\text{GHz}}^{\text{Max}}}$ (%) (4)	z (5)	ΔT^D (d) (6)	ΔF (Jy) (7)	σ (8)	F_{L} (Jy) (9)	F_{H} (Jy) (10)	ν (GHz) (11)	$\log T_{\text{B}}$ (K) (12)	δ (13)
0831+557	GAL	6.43	3.03	0.2412	60.03	0.67	0.11	5.25	5.92	4.8	14.34	2.94
0836+710	FSRQ	25.56	3.4	2.172	0.98	0.98	0.12	1.74	2.72	8	18.9	23.99
0838+133	FSRQ	14.17	5.29	0.684	1.01	0.99	0.1	0.72	1.71	14.5	17.8	14.45
0850+581	FSRQ	9.79	3.64	1.322	92.53	0.16	0.03	0.67	0.83	14.5	13.43	1.94
0851+202	BL	17.47	1.69	0.306	0.9	0.48	0.08	5.1	5.58	14.5	17.06	10.27
0859+470	FSRQ	12.43	11.62	1.462	64.03	0.18	0.03	0.91	1.09	14.5	13.85	2.35
0906+430	FSRQ	12.04	2.36	0.668	0.98	0.27	0.04	0.84	1.11	8	17.76	14.21
0912+297	BL	49.03	20.08		74.64	0.13	0.01	0.18	0.31	14.5	12.87	1.49
0917+458	N	8.66	1.41	0.1744	91.45	0.38	0.05	2.4	2.78	4.8	13.48	1.98
0917+624	FSRQ	14.23	8.6	0.7	1.07	0.28	0.05	1.35	1.63	4.8	18.17	17.17
0923+392	FSRQ	5.07	0.86	0.6948	0.96	0.74	0.09	8.82	9.56	4.8	18.69	21.74
0951+699	GAL	14.4	0.72	0.0009	2.01	0.27	0.04	1.53	1.8	14.5	11.22	0.7
0954+556	FSRQ	16.06	4.36	0.901	42.43	0.4	0.08	1.19	1.59	14.5	14.32	2.9
0954+658	BL	90.99	17.65	0.367	0.94	0.29	0.03	0.42	0.71	14.5	16.93	9.67
0957+227	BL	83.2	26.89	0.419	1.99	0.08	0.01	0.1	0.18	14.5	15.81	5.77
1003+351	FSRQ	9.11	2.52	0.0989	76.05	0.3	0.06	0.9	1.2	8	12.65	1.35
1031+567	GAL	19.39	8.06	0.459	2.59	0.37	0.07	0.49	0.86	8	16.82	9.21
1034–293	FSRQ	15.97	4.21	0.312	0.98	0.26	0.05	1.95	2.21	8	17.25	11.21
1038+528	FSRQ	17.99	7.01	2.296	7.98	0.09	0.01	0.62	0.71	4.8	16.51	7.97
1040+123	FSRQ	17.04	2.84	1.029	12.04	0.74	0.12	0.97	1.71	8	16.26	7.12
1055+018	FSRQ	12.77	3.39	0.888	0.97	0.58	0.09	3.66	4.24	8	18.27	17.92
1100+772	BL	63.9	10.53	0.311	89.57	0.58	0.11	0.16	0.74	8	13.67	2.16
1101+384	BL	20	2.99	0.031	0.52	0.12	0.02	0.61	0.73	14.5	15.1	4.17
1127–145	FSRQ	9.25	2.49	1.187	0.97	0.49	0.09	3.69	4.18	8	18.34	18.58
1133+704	BL	82.95	49.27	0.046	9.96	0.12	0.02	0.23	0.35	4.8	13.83	2.32
1137+660	FSRQ	65.83	70.92	0.6563	30.56	0.31	0.06	0.56	0.87	8	14.83	3.67
1147+245	BL	17.87	5.52	0.2	15.99	0.13	0.01	0.65	0.78	14.5	13.68	2.17
1156+295	FSRQ	13.11	1.32	0.729	0.98	0.1	0.01	0.81	0.91	14.5	16.87	9.41
1157+732	GAL	10.23	3.87	0.9737	82.6	0.49	0.09	1.44	1.93	8	14.38	3
1215+303	BL	54.7	50.16	0.237	2.02	0.18	0.03	0.25	0.43	4.8	16.7	8.72
1217+023	FSRQ	13.68	8.54	0.24	7.66	0.19	0.03	0.24	0.43	14.5	14.62	3.34
1219+285	BL	19.26	4.62	0.13	0.96	0.29	0.05	1.2	1.49	4.8	17.09	10.45
1222+216	FSRQ	5.67	1.15	0.435	1.99	0.37	0.05	1.86	2.23	14.5	16.5	7.93
1225+206	FSRQ	69.37	27.21	0.68	6.99	0.15	0.03	0.5	0.65	4.8	16.26	7.1
1226+023	FSRQ	6.67	0.12	0.158	0.94	1.67	0.31	31.48	33.15	4.8	18.03	16.05
1253–055	FSRQ	5.66	0.74	0.536	0.89	0.67	0.13	13.37	14.04	14.5	17.59	13.12
1254+476	GAL	12.87	2.21	0.996	65.98	0.42	0.07	0.84	1.26	8	14.52	3.2
1307+121	BL	22.5	5.82		1.09	0.19	0.04	0.82	1.01	8	17.22	11.09
1308+326	BL	13.19	5.74	0.996	0.96	0.44	0.09	3.92	4.36	8	18.22	17.52
1328+307	FSRQ	13.88	1.63	0.846	0.96	0.61	0.09	2.9	3.51	14.5	17.75	14.16
1335–127	FSRQ	8.05	0.43	0.539	0.92	0.59	0.08	6.24	6.83	14.5	17.51	12.64
1354–152	FSRQ	12.12	3.67	1.89	94.18	0.16	0.03	1.01	1.17	14.5	13.58	2.07
1358+624	GAL	25.8	11.56	0.431	14.49	0.2	0.03	0.49	0.69	14.5	14.5	3.16
1400+162	BL	42.38	26.31	0.245	92.53	0.28	0.04	0.09	0.37	8	13.15	1.7
1409+524	GAL	5.34	1.92	0.4614	41.46	0.27	0.05	3.62	3.89	8	14.28	2.86
1413+135	BL	21.5	9.54	0.247	0.96	0.39	0.07	1.66	2.05	14.5	16.76	8.94
1418+546	BL	36.86	17.95	0.151	0.93	0.5	0.06	1.56	2.06	8	17.03	10.15
1458+718	FSRQ	7.46	2.07	0.905	88.47	0.54	0.11	2.21	2.75	14.5	13.81	2.3
1504–166	FSRQ	10.24	2.94	0.876	2.94	0.24	0.04	2.45	2.69	4.8	17.36	11.79
1510–089	FSRQ	8.62	3.14	0.359	0.9	0.23	0.04	2.39	2.62	8	17.37	11.84
1514+197	BL	25.62	13.19	1.07	25.54	0.23	0.04	0.49	0.72	4.8	15.57	5.17
1538+149	BL	13.83	1.37	0.605	0.99	0.22	0.03	1.29	1.51	8	17.61	13.22
1543+005	N	21.23	14.71	0.55	75.58	0.16	0.03	0.63	0.79	14.5	13.13	1.68
1606+106	FSRQ	15.46	2.38	1.23	4.99	0.32	0.05	1.29	1.61	14.5	16.24	7.04
1609+660	GAL	11.8	2.52	0.549	60.03	0.19	0.04	2.15	2.34	4.8	14.36	2.96
1611+343	FSRQ	11.63	2.82	1.401	1	0.26	0.05	3.45	3.71	4.8	18.57	20.57
1624+416	FSRQ	12.02	5.79	2.55	0.97	0.28	0.04	0.92	1.2	8	18.42	19.27
1633+382	FSRQ	7.09	2.9	1.814	1.05	0.21	0.04	2	2.21	14.5	17.58	13.08
1634+628	FSRQ	15.29	9.44	0.988	69.6	0.15	0.03	0.38	0.53	14.5	13.51	2

Table 1 — *Continued.*

Name (B1950) (1)	ID (2)	$P_{8\,\mathrm{GHz}}^{\mathrm{Max}}$ (%) (3)	$\sigma_{P_{8\,\mathrm{GHz}}^{\mathrm{Max}}}$ (%) (4)	z (5)	ΔT^D (d) (6)	ΔF (Jy) (7)	σ (8)	F_{L} (Jy) (9)	F_{H} (Jy) (10)	ν (GHz) (11)	$\log T_{\mathrm{B}}$ (K) (12)	δ (13)
1637+574	FSRQ	15.04	7.31	0.7506	0.95	0.89	0.08	1.87	2.76	14.5	17.86	14.86
1641+399	FSRQ	7.4	1.32	0.594	0.98	0.29	0.06	5.01	5.3	8	17.72	13.95
1642+690	FSRQ	32.43	4.98	0.751	0.98	0.4	0.07	1.15	1.55	14.5	17.49	12.51
1652+398	BL	13.41	4.39	0.0337	0.9	0.47	0.08	1.41	1.88	8	15.8	5.76
1717+178	BL	39.71	23.37	0.114	71	0.28	0.03	0.78	1.06	14.5	12.28	1.14
1721+343	FSRQ	37.09	27.64	0.206	45.42	0.22	0.04	0.39	0.61	8	13.54	2.03
1727+502	BL	32.46	12.19	0.055	61.05	0.23	0.04	0.18	0.41	8	12.24	1.12
1730–130	FSRQ	8.19	0.71	0.9	0.99	0.66	0.1	4.58	5.24	8	18.31	18.31
1741–038	FSRQ	6.24	4.49	1.054	1.01	0.55	0.09	3.92	4.47	14.5	17.78	14.34
1749+096	BL	11.47	0.94	0.322	0.96	0.26	0.04	2.69	2.95	4.8	17.73	14
1749+701	BL	46.46	11.54	0.77	0.92	0.38	0.06	0.31	0.69	4.8	18.49	19.89
1803+784	BL	11.27	2.74	0.679	0.97	0.67	0.07	1.7	2.37	14.5	17.66	13.55
1807+698	BL	9.5	0.93	0.051	2.07	0.4	0.04	1.58	1.98	8	15.36	4.7
1823+568	BL	18.35	2.55	0.6635	1.99	0.4	0.06	1.62	2.02	14.5	16.8	9.11
1828+487	FSRQ	3.15	1.33	0.691	2.82	0.36	0.06	4.08	4.44	14.5	16.47	7.85
1842+455	GAL	17.03	4.77	0.0908	73.62	0.11	0.01	0.52	0.63	14.5	11.66	0.85
1845+797	GAL	10.61	1.35	0.0569	0.95	0.55	0.07	2.23	2.78	14.5	15.75	5.62
1901+319	FSRQ	9.57	4.12	0.635	1	0.28	0.05	1.67	1.95	8	17.73	14
1921–293	FSRQ	5.73	1.08	0.352	0.6	1.34	0.2	8.39	9.73	8	18.47	19.68
1928+738	FSRQ	6.16	2.11	0.36	0.97	0.24	0.04	2.65	2.89	14.5	16.81	9.14
1939+605	GAL	19.01	2.28	0.201	88.62	0.2	0.04	1.51	1.71	4.8	13.34	1.85
1951+498	FSRQ	44.72	28.73	0.466	0.99	0.47	0.08	0.18	0.65	8	17.77	14.25
1954+513	FSRQ	11.51	4.71	1.23	17.55	0.4	0.06	0.98	1.38	14.5	15.24	4.45
2005+403	FSRQ	7.93	2.83	1.736	1	0.46	0.06	3.02	3.48	8	18.46	19.63
2007+777	BL	12.72	7.38	0.342	0.15	0.23	0.04	2.56	2.79	14.5	18.37	18.81
2014+370	N	9.91	1.13		17.66	0.24	0.04	0.81	1.05	14.5	14.76	3.56
2020+614	GAL	3.91	2.78		3.07	0.34	0.05	2.17	2.51	14.5	15.94	6.13
2032+107	BL	34.83	15.76	0.601	38.48	0.23	0.04	0.51	0.74	14.5	13.93	2.43
2121+053	FSRQ	14.38	8.61	1.941	1.01	0.41	0.08	3.35	3.76	8	18.45	19.51
2131–021	BL	12.07	4.87	1.285	0.99	0.3	0.06	1.79	2.09	8	18.15	17
2134+004	FSRQ	7.3	0.85	1.932	0.92	0.87	0.15	8.39	9.26	8	18.86	23.52
2136+141	FSRQ	3.59	1.08	2.427	6.98	0.13	0.02	1.51	1.64	14.5	15.84	5.87
2145+067	FSRQ	4.42	1.95	0.99	0.89	1.55	0.1	7.7	9.25	14.5	18.31	18.29
2153+377	GAL	17.46	3.31	0.292	0.98	0.48	0.09	0.88	1.36	8	17.47	12.4
2155–152	FSRQ	15.3	1.13	0.672	1.02	0.42	0.05	2.36	2.78	4.8	18.37	18.77
2155–304	BL	61.71	21.5	0.116	0.99	0.37	0.07	0.17	0.54	8	16.64	8.47
2200+420	BL	14.83	1.56	0.0688	0.88	0.47	0.08	3.18	3.65	14.5	15.9	6.04
2202+315	FSRQ	6.07	0.86		0.93	0.22	0.04	2.27	2.49	14.5	17.43	12.22
2223–052	FSRQ	7.69	2.08	1.404	1	0.81	0.08	5.69	6.5	4.8	19.06	25.82
2229+391	GAL	16.39	5.88	0.0171	99.59	0.25	0.04	1.11	1.36	4.8	11.31	0.73
2230+114	FSRQ	10.45	2.82	1.037	0.89	0.42	0.06	3.09	3.51	14.5	17.77	14.24
2243+394	GAL	13.26	1.98	0.811	94.14	0.28	0.05	1.57	1.85	8	13.93	2.43
2251+158	FSRQ	5.78	0.29	0.859	0.99	0.77	0.11	10.62	11.39	14.5	17.84	14.71
2254+074	BL	30.36	15.09	0.19	9.95	0.19	0.03	0.24	0.43	4.8	15.18	4.32
2311+612	N	1.73	0.35		0.99	1.88	0.23	11.81	13.69	14.5	18.16	17.03
2335+031	GAL	30.87	24.07	0.31	92.56	0.24	0.03	0.35	0.59	8	13.26	1.78
2345–167	FSRQ	8.91	2.96	0.576	0.98	0.58	0.09	1.86	2.44	8	18.01	15.89
2351+456	FSRQ	24.64	1.98	1.992	0.99	0.14	0.02	0.83	0.97	14.5	17.5	12.57
2352+495	FSRQ	12.94	1.23	0.237	4.57	0.27	0.03	0.31	0.58	14.5	15.21	4.39

Col. (1) name of the source (B1950); Col. (2) the classification, BL is for a BL Lacertae object, FSRQ for flat spectrum radio quasar, GAL for a galaxy, and N for unidentified sources; Col. (3) the maximum polarization at 8 GHz; Col. (4) the uncertainty for the maximum polarization; Col. (5) the redshift; Col. (6) the short term timescale; Col. (7) the variability of flux; Col. (8) the error of Col. (7); Col. (9) low flux density corresponding to the short term timescale; Col. (10) high flux density corresponding to the short term timescale; Col. (11) frequency at which the variability timescale is determined; Col. (12) the brightness temperature and Col. (13) the boosting factor (δ).

In the present work, we choose Δt_{jk} as the timescale if $\Delta F_{jk} \geq 5\sqrt{\sigma_i^2 + \sigma_k^2}$. This critical value is used in the optical variability consideration by Xie et al. (1994), who used timescales corresponding to $\Delta m \geq 5\sigma_{max}$ as reasonable ones. Romero et al. (1999) used a 99% confidence criterion $C = \frac{\sigma_{O-C}}{\sigma_{C1-C2}}$ to check whether there is real variation. If the parameter $C \geq 3$, then the variation is true. In our consideration, we take the variation of $\Delta F_{ij} \geq 5\sqrt{\sigma_1^2 + \sigma_2^2}$ as a true variation, which shows high confidence. So, we take the timescale corresponding to the variation as the true timescale.

In our consideration, we found that the timescales range from 0.15 d (2007+777) to 176.2 d (0528–250) with an averaged timescale of $\Delta t_{ob} = 17.1 \pm 16.5$ d. We also found that most of the present sources have timescales less than 50 d. The present method is different from that used in the work by Aller et al. (1999) and Hughes et al. (1992), but our results do not conflict with those obtained by those authors.

The available data and the estimated brightness temperature are shown in Table 1. The brightness temperature (T) ranges (in log scale) from 10.47 K for 0316+416 to 19.06 K for 2223–052. Furthermore, the brightness temperatures are very high for some sources, but this is reasonable. Some sources show even higher brightness temperatures. For example, $\log T_B = 21$ K for 0537–441 (Romero et al. 1994) and $\log T_B = 17 \sim 19$ K for 0917+624 (Witzel & Quirrenbach 1993). The high temperature perhaps indicates a strongly beamed effect. If we consider the inverse Compton catastrophe ($T \leq 10^{12}$ K) (Kellermann & Pauliny-Toth 1969) for those sources, then the Doppler factor can be estimated from the brightness temperature as $\delta = [\frac{T_{ob}}{10^{12}}]^{1/3}$. Thus, the Doppler factor obtained is in the range: $\delta = 0.31$ for 0315+416 to $\delta = 225.63$ for 2223–052. The estimated Doppler factor for 2223–052 is too large. Qian et al. (1991) pointed out that the shocked jet models with peculiar geometries can reduce the requirement for the Doppler factor. In the case of a relativistic shock moving along the line of sight through inhomogeneous, small-scale structure distributed along the jet, the brightness temperature is transformed as $\delta^{-3}\gamma^{-2}$. If the viewing angle is small ($\cos\theta \sim \beta$), the required Doppler factor for the emitting region is $\sim (\frac{T_{obs}}{10^{12}})^{1/5}$ (Romero et al. 1994). In this case, we get the Doppler factors to be in the range of $\delta = 0.49$ to 25.82 (see Col. 11 in Table 1 for details), which is in the range of the Doppler factor $\delta = 0.04$ to 43 given by Ghisellini et al. (1993) and the results of $\delta = 0.3$ to 26 given by Lähteenmäki & Valtaoja (1999).

3.2 Interstellar Scintillation

In radio sources, radio variability, particularly rapid variability, can be caused by interstellar scintillation (ISS). The timescales caused by ISS are on the order of days, say 5 to 50 d (Heeschen et al. 1987; Quirrenbach et al. 1992; Lallement et al. 1992; Jauncey et al. 2003; Bignall et al. 2003; Bignall et al. 2006; Rickett et al. 2006). Rickett et al. (2006) found that the fast variations are relatively strong at 2 GHz and much weaker at 8 GHz. This is consistent with the expected decrease in ISS amplitude with increasing frequency. Therefore, the rapid variations found in the lower frequency light curves may be caused by ISS while the slower (year-long) variation frequencies are intrinsic.

Our results show that the timescales vary from 0.15 d to 176.2 d (0.5 yr), among which 143 sources have timescales less than 50 d (about 86% of all 166 sources). So, most of our timescales exclude the intrinsic variations. The timescales of those 143 sources might come from interstellar scintillation, but we cannot see this clearly. Because we do not find any dependence of the strength of intraday variations on galactic latitude, the effect is also not confined to a certain region in the sky (Quirrenbach et al. 1992).

Furthermore, 2223–052 has the highest brightness temperature ($\log T_B = 19.06$ K), which is greatly in excess of the Compton limit of about 10^{12} K. If we do not consider the influence of shocked jet models, then the Doppler factor can be 225.63. For this high temperature and high Doppler factor, there are two different explanations: intrinsic variation and refractive interstellar scintillation (Quirrenbach et al. 1992). The effect of intrinsic variation, with a high Doppler factor and noncausal effects (e.g. instantaneous interaction of preexisting "clouds" and shocks), should be considered (Quirrenbach et al. 1992), and gravitational microlensing might be another explanation (Gopal-Krishna & Subramanian 1991). The intrinsic variation can reach amplitudes of 20% or more, but 2223–052 only has 8.6%, so the intra-day variation of 2223–052 probably comes from interstellar scintillation.

3.3 Doppler Boosting Factor

For comparison, in Figure 3, we have plotted our results (δ_R) vs. those by Lahteenmark & Valtaoja (1999)–(δ_{LV}) and Ghisellini et al. (1993)–(δ_G). As is seen in Figure 3, in general, our estimates of the Doppler factor are similar to those by Lahteenmark & Valtaoja (1999) and Ghisellini et al. (1993). We can obtain $\delta_R = 0.36 \times \delta_{LV} + 10.39, p = 0.01$, and $\delta_R = 0.44 \times \delta_G + 8.5, p < 0.001$. The different results between our work and that by Ghisellini et al. (1993) is from the different methods. The difference between our result and that by Lahteenmark & Valtaoja (1999) is perhaps because of two reasons. 1. We used the intrinsic brightness temperature of 10^{12} K while Lahteenmark & Valtaoja (1999) used 5×10^{10} K, which makes our values about half of their values, $\delta_{5 \times 10^{10}} = 1.82 \times \delta_{10^{12}}$. 2. The small viewing angle ($\cos \theta \sim \beta$) is not always reasonable for the whole sample.

If we considered the BLs, FSRQs, and galaxies separately, we have δ = 1.02 to 19.89 with an average value of $\langle \delta \rangle = 8.7 \pm 5.4$ for BLs (or $\langle \delta \rangle = 8.5 \pm 5.3$ for the 47 BLs when the unknown redshift sources are included), δ = 1.34 to 25.82 with an average value of $\langle \delta \rangle = 12.19 \pm 6.45$ for FSRQs (or $\langle \delta \rangle = 12.29 \pm 6.45$ when the unknown redshift sources are included), δ = 0.49 to 12.39 with an average value of $\langle \delta \rangle = 3.97 \pm 3.22$ for galaxies. The relation between BLs and FSRQs is often discussed, hence for comparison, we carried out a K-S test on the distributions of their Doppler factors, and find, as shown in Figure 4, that the probability of Doppler factors of both BLs and FSRQs being from the same parent population is $p = 2.4 \times 10^{-3}$.
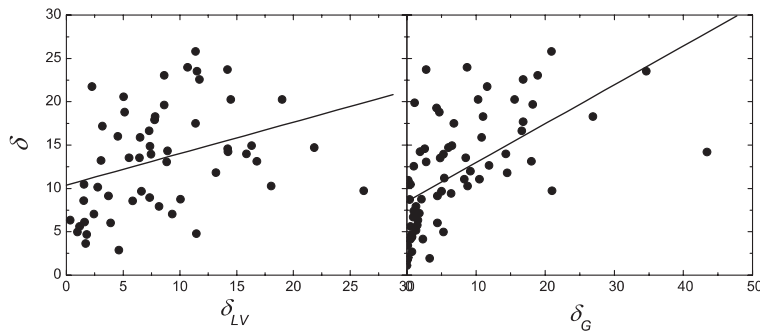
Fig. 3 Comparison between the Doppler factor estimated in the present work with those estimated by others. The left panel displays our results (δ) vs. Lahteenmark & Valtaoja (1999) (δ_{LV}) and the right panel displays our results (δ) vs. Ghisellini et al. (1993) (δ_G).
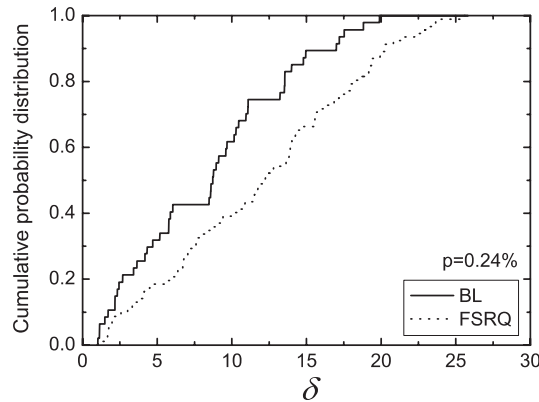
**Fig. 4** K-S test result of Doppler factor for BL Lacertae objects and FSRQs.

3.4 Polarization

High and variable polarization is one of the characteristics of blazars, which can be seen from the radio polarization database of UMRAO. Based on a two-component beaming model (Urry & Shafer 1984; see also Urry & Padovani 1995), the emission from an AGN has two components, namely beamed and unbeamed. Assuming the intrinsic flux of the jet, $F_j^{\rm in}$, to be a fraction f of the unbeamed flux, $F_{\rm unb}$, i.e., $F_j^{\rm in} = f F_{\rm unb}$, one can get $F^{\rm ob} = F_{\rm unb} + F_j^{\rm ob} = (1 + f\delta^p)F_{\rm unb}$. If one assumes that the emission in the co-moving jet is also composed of two components, namely the polarized and the unpolarized, with the two components being proportional to each other, $F_j^{\rm in} = F_j^p + F_j^{\rm up}$ and $F_j^p = \eta F_j^{\rm up}$, then a relation between the observed polarization and the Doppler factor can be obtained (Fan et al. 1997; see also Fan et al. 2001, 2006).

$$P^{\rm ob} = \frac{f\delta^p}{1 + f\delta^p}\frac{\eta}{1 + \eta}, \tag{3}$$

where δ is the Doppler factor, and η is the ratio of the polarized to the unpolarized luminosity in the jet.

The maximum polarization values are available at three frequencies, but for our consideration, we have used the values at 8 GHz. Using the observed maximum polarization to get the diagram of polarization against Doppler factor, we find that the observation points fit the theoretical curves well (see Fig. 5), suggesting an association between the relativistic boosting effect and polarization.
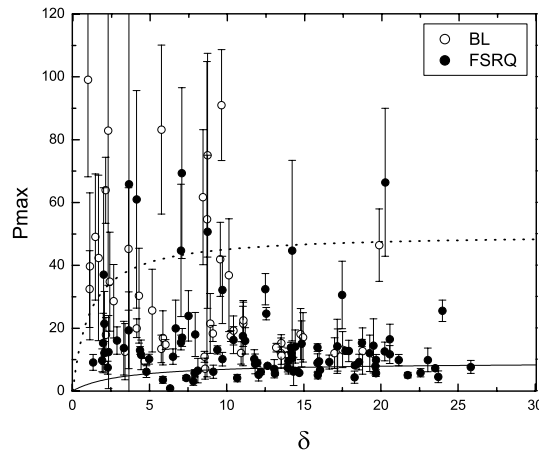
Fig. 5 Plot of the maximum polarization at 8 GHz against the radio Doppler factor estimated in the present work. The filled points stand for FSRQs, the circle points for BLs; the lower curve represents η = 0.1 and f = 0.3, the upper curve η = 1.0 and f = 0.9.

4 CONCLUSIONS

In this paper, based on the UMRAO database, we have determined short-term variability timescales, which in turn were used to calculate the brightness temperature and then estimate the corresponding Doppler factors for 166 sources. We found that 1) The timescales are 0.15 d (2007+777) to 176.17 d (0528−250) with an average timescale of $\Delta t_{\rm ob}$ = 17.5 ± 16.5 d for the whole sample; 2) The brightness temperatures, $T_{\rm B}$ are in the range of log $T_{\rm B}$ = 10.47 to 19.06 K; and 3) The Doppler factors are in the range of 0.5 to 25.82. Finally, we discussed the association between the Doppler factor and polarization; the result suggests that polarization is associated with the relativistic beaming model.

References

Agudo, I., Bach, U., Krichbaum, T. P., et al. 2007, A&A, 476, L17
Aller, M. F., Aller, H. D., & Hughes, P. A. 2003, ApJ, 586, 33
Aller, M. F., Aller, H. D., Hughes, P. A., & Latimer, G. E. 1999, ApJ, 512, 601
Aller, M. F., Aller, H. D., & Hughes, P. A. 1992, ApJ, 399, 16
Andruchow, I., Romero, G. E., & Cellone, S. A. 2005, A&A, 442, 97
Bignall, H. E., Jauncey, D. L., Lovell, J. E. J., et al. 2003, ApJ, 585, 653
Bignall, H. E., Macquart, J. P., Jauncey, D. L., et al. 2006, ApJ, 652, 1050
Cellone, S. A., Romero, G. E., Combi, J. A., & Martí, J. 2007, MNRAS, 381, L60
Cheng, K. S., Fan, J. H., & Zhang, L. 1999, A&A, 352, 32
Ciprini, S., Takalo, L. O., Tosti, G., et al. 2007, A&A, 467, 465
Dondi, L., & Ghisellini, G. 1995, MNRAS, 273, 583
Efimov, Y. S., Shakhovskoy, N. M., Takalo, L. O., & Sillanpaa, A. 2002, A&A, 381, 408
Fan, J. H. 2005a, ChJAA (Chin. J. Astron. Astrophys.), 5S, 213
Fan, J. H. 2005b, A&A, 436, 799
Fan, J. H., et al. 2006, ChJAA (Chin. J. Astron. Astrophys.), 6S2, 349
Fan, J. H., Wang, Y. J., Yang, J. H., & Su, C. Y. 2004, ChJAA (Chin. J. Astron. Astrophys.), 4, 533
Fan, J. H., Cheng, K. S., & Zhang, L. 2001, PASJ, 53, 201
Fan, J. H., Xie, G. Z., & Bacon, R. 1999, A&AS, 136, 13
Fan, J. H., Cheng, K. S., Zhang, L., & Liu, C. H. 1997, A&A, 327, 947
Fan, J. H., Xie, G. Z., & Wen, S. L. 1996, A&AS, 116, 409
Gaidos, J. A., et al. 1996, Nature, 383, 319
Ghisellini, G., Padovani, P., Celotti, A., & Maraschi, L. 1993, ApJ, 407, 65
Gopal-Krishna, R., & Subramanian, K. 1991, Nature, 349, 766
Gupta, A. C., Banerjee, D. P. K., Ashok, N. M., & Joshi, U. C. 2004, A&A, 422, 505
Heeschen, D. S., Krichbaum, T., Schalinski, C. J., et al. 1987, AJ, 94, 1493
Hughes, P. A., Aller, H. D., & Aller, M. F. 1992, ApJ, 396, 469
Jauncey, D. L., Johnston, H. M., Bignall, H. E., et al. 2003, Ap&SS, 288,63
Kellermann, K. I., & Pauliny-Toth, I. I. K. 1969, ApJ, 155, L71
Kovalev, Y. A., & Kovalev, Y. Y. 2006, ASPC, 360, 137
Lallement, R., & Bertin, P. 1992, A&A, 266, 479
Lind, K. R., & Blandford, R. D. 1985, ApJ, 295, 358
Lähteenmäki, A., & Valtaoja, E. 1999, AJ, 117, 1168
Qian, S. J., Quirrenbach, A., Witzel, A., et al. 1991, A&A, 241, 15
Quirrenbach, A., Witzel, A., Krichbaum, T. P., et al. 1992, A&A, 258, 279
Rickett, B. J., Lazio, T. J. W., Chigo, F. D., et al. 2006, ApJS, 165, 439
Romero, G. E., Combi, J. A., & Colomb, F. R. 1994, A&A, 288, 731
Romero, G. E., Cellone, S. A., & Combi, J. A. 1999, A&AS, 135, 477
Romero, G. E., Cellone, S. A., Combi, J. A., & Andruchow, I. 2002, A&A, 390, 431
Sambruna, R. M., Chou, L. L., & Urry, C. M. 2000, ApJ, 533, 650
Urry, C. M., & Padovani, P. 1995, PASP, 107, 803
Urry, C. M., & Shafer, R. A. 1984, ApJ, 280, 569
Vermeulen, R. C., et al. 1995, ApJ, 452, L5
Wagner, S. J., & Witzel, A. 1995, ARA&A, 33, 163
Wills, B. J., Wills, D., Breger, M., et al. 1992, ApJ, 398, 454
Witzel, A., & Quirrenbach, A. 1993, Propagation Effects in Space VLBI, 33
Xie, G. Z., Liu, F. K., Liu, B. F., et al. 1991, A&A, 249, 65
Xie, G. Z., Li, K. H., Zhang, Y. H., et al. 1994, A&AS, 106, 361
Xie, G. Z., et al. 2004, MNRAS, 348, 831